J Exp Biol Advance Online Articles. First posted online on 8 June 2017 as doi:10.1242/jeb.160234
Access the most recent version at http://jeb.biologists.org/lookup/doi/10.1242/jeb.160234

Chamber music – An unusual Helmholtz resonator for song amplification in a Neotropical bush-cricket (Orthoptera, Tettigoniidae)

Thorin Jonsson[1*], Benedict D. Chivers[1], Kate Robson Brown[2], Fabio A. Sarria-S[1], Matthew Walker[1] and Fernando Montealegre-Z[1*]

[1]School of Life Sciences, Joseph Banks Laboratories, Green Lane, Lincoln, LN6 7DL, UK
[2]Imaging Laboratory, Department of Anthropology and Archaeology, University of Bristol, 43 Woodland Road, Bristol, BS8 1UG, UK

*Authors for correspondence (fmontealegrez@lincoln.ac.uk, tjonsson@lincoln.ac.uk)

Keywords: Acoustic resonator, bush-cricket, bioacoustics, laser Doppler vibrometry, finite element modelling, micro computed tomography.

Journal of Experimental Biology • Advance article

Summary statement

We use laser vibrometry, micro computed tomography and finite element modelling to show that an unusual pronotal inflation covering the wings of a bush-cricket acts as a Helmholtz resonator.

Abstract

Animals use sound for communication, with high-amplitude signals being selected for attracting mates or deterring rivals. High amplitudes are attained by employing primary resonators in sound producing structures to amplify the signal (e.g., avian syrinx). Some species actively exploit acoustic properties of natural structures to enhance signal transmission by using these as secondary resonators (e.g., tree-hole frogs). Male bush-crickets produce sound by tegminal stridulation and often use specialised wing areas as primary resonators. Interestingly, *Acanthacara acuta*, a Neotropical bush-cricket, exhibits an unusual pronotal inflation, forming a chamber covering the wings. It has been suggested that such pronotal chambers enhance amplitude and tuning of the signal by constituting a (secondary) Helmholtz resonator. If true, the intact system – when stimulated sympathetically with broadband sound – should show clear resonance around the song carrier frequency which should be largely independent of pronotum material, and change when the system is destroyed. Using laser Doppler vibrometry on living and preserved specimens, micro computed tomography, 3D printed models, and finite element modelling, we show that the pronotal chamber not only functions as a Helmholtz resonator due to its intact morphology but also resonates at frequencies of the calling song on itself, making song production a three-resonator system.

Journal of Experimental Biology • Advance article

Introduction

Acoustic communication plays a vital role in the life of many animals as a means to attract and locate potential mating partners or deter rivals (e.g. (Drosopoulos and Claridge, 2006; Hauser, 2000; Hedwig, 2014)). Loud signals are often positively selected for since high amplitude sounds can reach more potential mating partners and contain information about the sender's fitness (e.g. (Marten et al., 1977; Prestwich, 1994)). For small vertebrates and insects, the production of high amplitude communication signals is often a morphological challenge due to the power and size of their sound production mechanisms (Bennet-Clark, 1998; Prestwich, 1994). Many animals therefore produce sounds by coupling the initial sound producing structures to mechanical resonators that increase the amplitude of the generated sound at and around their resonant frequencies (Fletcher, 2007). This also serves to increase the sound radiating area, which increases impedance matching between the structure and the surrounding medium (Bennet-Clark, 2001). Common examples of these kinds of primary resonators are the avian syrinx (Fletcher and Tarnopolsky, 1999) or the cicada tymbal (Bennet-Clark, 1999). In addition to primary resonators, some animals have developed morphological or behavioural adaptations that act as secondary resonators, further amplifying acoustical vibrations and facilitating sound radiation. The Bornean tree-hole frog *Metaphrynella sundana*, for example, adapts the frequency of his calls to the resonance of the tree trunk cavities it sings from, thereby increasing call amplitude (Lardner and bin Lakim, 2002), while the bladder cicada *Cystosoma saundersii* uses an internal air sac as secondary resonator (Bennet-Clark and Young, 1994) and mole crickets (*Neoscapteriscus borellii*, formerly *Scapteriscus acletus*) sing from horn-shaped burrows to amplify their songs (Bennet-Clark, 1987).

In the Ensifera (crickets, bush-crickets and allies), it is generally the male that produces acoustic mating signals by stridulating with their fore wings, while the (mostly) silent female receives the song and performs phonotactic movements towards the sender (e.g. (Kalmring et al., 2003; Robinson and Hall, 2002)). In bush-crickets, stridulation involves a serrated vein (the file) on the underside of the left wing which is swept over a hardened part of the anal edge (the plectrum) of the right wing, creating a series of oscillatory impacts that are sustained and amplified by specialised resonating wing areas (the primary resonators), like the mirror (Montealegre-Z, 2009; Montealegre-Z and Postles, 2010; Morris, 1999; Robinson and Hall, 2002). While crickets and humpbacked crickets use coupled radiators in symmetric wings for sound radiation (Bennet-Clark, 2003; Chivers et al., 2015; Masaki et al., 1987; Montealegre-Z et al., 2011), male bush-crickets exhibit conspicuous wing asymmetry, with the sound radiators of the file-bearing wing being thicker and acoustically more damped than the plectrum bearing wing (Chivers et al., 2014; Montealegre-Z and Mason, 2005; Sarria et al., 2016). This morphological and functional asymmetry results in the loss of an acoustic radiator, and different bush-cricket species have evolved various forms to compensate for this situation (Bennet-Clark, 1998). For example, wing inflations (Heller et al., 2010), thorax depression (Braun et al., 2009; Morris et al., 2016) and pronotal covers (Morris and Mason, 1995).

In most species of tettigonids, the pronotum is flat and either leaves the stridulum on the fore wings free, or only partly covers them, so the produced sound signals are radiated unhindered or slightly baffled (although, see (Rentz, 1988) for notable exceptions in the Arytropteridini of the Tettigoniinae). In contrast to this, males of the Neotropical bush-cricket *Acanthacara acuta* (Tettigoniidae, Conocephalinae, Cestrophorini) possess an unusually inflated pronotum that stretches posteriorly to cover the entirety of the short, brachypterous wings and the first abdominal segment (Fig. 1). The extent of this pronotal inflation is such that it covers the dorsal half of the thorax laterally and either encloses the wings completely, or only leaves a small opening at the posterior part, depending on posture. This inflation thus resembles a cave or chamber and is therefore called the pronotal chamber (PC) from here on.

Journal of Experimental Biology • Advance article

Since male *A. acuta* are small (~2 cm) but produce very loud calling songs (85 dB SPL re 20 µPa at 10 cm (Morris and Mason, 1995)) and females do not exhibit an inflated pronotum (Gurney, 1972), it seems very likely that the PC is connected to sound production and serves to amplify and/or direct the song to increase male courtship success. Indeed, Morris & Mason, 1995 (Morris and Mason, 1995) investigated the role of the PC and the possibility that it could function as a (secondary) Helmholtz resonator, thereby greatly amplifying and filtering the acoustic output. While Morris and Mason's research showed that the PC of *A. acuta* does amplify and sharpen the produced songs when compared to songs that were produced by males with the chamber removed, they only provided estimates for morphological properties of the chamber and therefore only concluded that its "function as a Helmholtz resonator is plausible" (Morris and Mason, 1995).

In a Helmholtz resonator, a volume of gas (usually air) in a confined space with a small opening (e.g. a neck or a hole) is set into motion by a driving force whereby the gas is either compressed or rarefied. This creates either a high or low pressure field expelling or pulling in air through the opening. Due to the flowing gas' momentum, the pressure field does not equalise to the surrounding pressure but reverses, creating a low pressure field where gas is pushed out and a high pressure field where it is pulled into the confined space. Once set in motion, this process repeats in an oscillatory fashion, like a mass on a spring, where the frequency of oscillation – the resonance of the system – is dependent on the volume and density of the gas and the size and height of the opening and largely independent on the structural material (Bennet-Clark, 1999; Fletcher and Rossing, 1998). Well known examples of Helmholtz resonant systems are the air cavities in musical instruments like the guitar and violin, and when blowing air across the top of an empty bottle to create low frequency tones (von Helmholtz, 1863).

If the PC of *A. acuta* is indeed a Helmholtz resonator for the calling song, it should show resonance at the song's carrier frequency (CF) when stimulated non-invasively with broadband sound. This resonance frequency should match with theoretical Helmholtz resonance calculations using the chamber's geometrical dimensions, and should be independent of the chamber material. Furthermore, removing the PC from the insect should destroy the Helmholtz resonator and change the chamber's resonance, revealing the material's vibratory properties.

Using scanning laser Doppler vibrometry (LDV), micro computed tomography (µ-CT), 3D printed models of the insects, and finite element modelling (FEM), this research is designed to show that the pronotal chamber of *A. acuta* not only resonates at the male's song frequencies but also acts as a Helmholtz resonator, due to its morphological dimensions and structure.

Materials and methods

Animals

Five *Acanthacara acuta* Scudder males were collected in Ecuador (Santa Lucía Cloud Forest Reserve, Barrio La Delicia, Nanegal, Pichincha, Ecuador, September 10th-20th, 2014) and transported to Lincoln, UK, where they were kept in climate controlled chambers (16°C, 70% RH, 12h:12h D:N cycle) until experiments were performed. Animals were fed *ad libitum* with apple, baby corn and fish flakes (Sinclair Animal & Household Care Ltd., Gainsborough, UK). One pinned specimen (provided by Glenn Morris, University of Toronto) was collected in Bellavista, Ecuador in 1988. All experiments were carried out on these six specimens.

Song recordings

Of the five specimens collected, songs of four freely behaving males were recorded in the field (18°C) using a Tascam DR-05 Version 2 Dictaphone Linear PCM Portable Recorder (TEAC Corporation, Tokyo, Japan) and saved at 96 kHz sampling rate.

The remaining male was recorded in the lab (temperature 23-26° C) with a 1/8" Brüel & Kjær Type 4138 condenser microphone, connected to a Brüel & Kjær 2633 preamplifier (Brüel & Kjær, Nærum, Denmark). Signals were recorded via the LDV internal data acquisition board (National Instruments PCI-4451; Austin, TX, USA) and stored as text files (96 kHz sampling rate) for later analysis with MATLAB (R2014a, MathWorks, Inc., Natick, USA). Spectral analysis was performed on recorded song pulses using power spectral density estimates (discrete Fourier transform, nfft=1024 points, Δf=94 Hz) over each pulse. Averages for the carrier frequency (CF) were calculated for each individual and the resulting means were pooled to gain an overall mean and standard deviation (SD, see Table S1).

Laser Doppler vibrometry

Pronotum resonances

To obtain the resonance properties of the wings and the PC, we used micro-scanning laser Doppler vibrometry (PSV-F-500 laser Doppler vibrometer; Polytec, Waldbronn, Germany; see (Montealegre-Z et al., 2011) for a detailed description) to measure the vibration velocities and displacements of these structures in response to stimulation with broadband periodic chirps. In short, animals were positioned and fixed with metal clamps on a small, custom-built holder with the thorax bent forward so that the entire chamber entrance is exposed, as when singing naturally. The entire dorsal and lateral surfaces of the PC were scanned while moving the laser beam around the specimen and keeping the speaker in a fixed position dorsal to the specimen. Broadband audio chirps (2-100 kHz) were generated by the PSV-500 acquisition board and transmitted to an ultrasound loudspeaker (Avisoft Vifa, Avisoft, Glienicke, Germany) positioned 30 cm away from the animal via an amplifier (A-400, Pioneer, Kawasaki, Japan). The speaker output was flattened to broadcast all frequencies at equal amplitudes (± 3 dB SPL) at the wings as measured by a calibrated reference microphone (see above). Vibrations, reference stimulus and internally calculated transfer functions of the measured vibration relative to the measured sound pressure were recorded at 256 kHz sampling rate (Δf=15.6 Hz; see Montealegre-Z et al., 2011 for details) and analysed and stored using PSV 9.0 (Polytec, Waldbronn, Germany). Experiments were carried out on four of the collected animals and one preserved specimen at temperatures between 23-26° C.

Wing resonances

After these recordings, the chamber was removed using micro-dissection tools exposing the wings fully. Wings were elevated and fixed in position with a drop of wax at the base of the axillary sclerites and scanned using LDV as described above (see also (Chivers et al., 2017; Montealegre-Z et al., 2011; Sarria et al., 2016)).

Vibration of isolated pronota

To investigate the vibrational properties of the PC itself, two pronota dissected from two living specimens were scanned using LDV. Removed pronota were fixed at the anterior end on a small pin using bees wax. Results should provide vibrational characteristics of the open cuticular structure, unimpeded by thorax and abdomen. If results from the intact PC are to some degree due to Helmholtz resonance, the removed chamber vibrations should show marked differences. Also, since Helmholtz resonance is not influenced by material properties (here the hard cuticle of the pronotum and the softer cuticle of the thorax and abdomen), it should be possible to restore the original vibrational patterns by artificially sealing the ventral side (or groove) of the removed PC, recreating the original dimensions of the resonator. In order to test this, the ventral side of the PC was covered with Blu-tack (Bostik Ltd, Leicester, UK) to approximately achieve a similar internal volume and opening as in the natural condition. This sealed PC was then rescanned using LDV.

Vibration of synthetic 3D-printed pronotum

In addition, one 1:1 scale model of *A. acuta* was 3D-printed and subjected to LDV recordings to investigate the resonances of the PC when made of artificial materials (see below). The model was fixed to holder and scanned using LDV and acoustic stimulation as described above.

µ-CT

X-ray microcomputer tomography (µ-CT) of one adult *A. acuta* male was performed using a SkyScan 1172 µ-CT scanner (Bruker Corporation, Billerica, MA, USA) with a resolution of 10 µm (50 kV source voltage, 200 µA source current, 420 ms exposure and 0.6° rotation steps). Before the µ-CT scan, the animal was asphyxiated with ethyl ethanoate (ethyl acetate; Sigma-Aldrich Company Ltd., Dorset, UK), placed upright in a small Eppendorf tube and positioned in a custom built holder in the CT scanner. µ-Ct projection images were reconstructed to produce stacks of orthogonal slices with NRecon (v. 1.6.9.18, Bruker Corporation, Billerica, MA, USA), stacks were processed with CTAn (v. 1.15.4, Bruker Corporation) and virtual 3D models were built from the resulting images using Avizo (v. 8.0, FEI, Hillsboro, USA). Models were 3D printed on a Form 1+ (Formlabs Inc, USA) with a layer thickness of 25 µm, using white resin (White Resin Version 2, Formlabs Inc, USA).

Finite element modelling

After creating models of the animal, its wings and PC, the surface geometry of the latter was saved in STL format and post-processed in 3ds Max 2015 (Autodesk, Inc., San Rafael, USA) to ensure fidelity of the geometry. The model was then used to carry out the FEM to resolve the PC eigenfrequencies and frequency responses using Comsol (v. 5.2a, Comsol, Inc., Burlington, USA).

Here, the chamber was modelled as a simple shell structure coupled to an acoustic pressure air domain with the following material properties: Young's modulus E=8 GPa; Poisson's ratio ν=0.33; cuticle density ρ=1200 kg/m^3 (values taken from (Klocke and Schmitz, 2011; Malkin et al., 2014; Vincent and Wegst, 2004)). Values for Young's modulus for insect cuticle in the literature range from several 100 MPa to ca. 50 GPa, depending on the species, the structure investigated and method used (Klocke and Schmitz, 2011; Smith et al., 2000; Vincent and Wegst, 2004). Since no data for the pronotum of any bush cricket or comparable insect could be found, the value of 8 GPa was chosen as reported for tibia cuticle in (Vincent and Wegst, 2004).

Frequency responses of the chamber to sound were modelled by placing a dipole point sound source (with a fixed 1e-6 N force vector pointing dorsally, resulting in a sound pressure level of ca. 98 dB at the source) into the middle of the chamber model, approximately where the wing resonators would be localised in the animal. Using parametric sweeps, the response of the chamber to sine wave pure tones at a range of frequencies (2-40 kHz at 50 Hz intervals) was analysed.

The finished model had 1894 meshed faces with an average element quality of 0.95±0.05 and an average face size of 0.040±0.009 mm^2. An increase in the number of meshed elements for the model did not significantly alter the computational results (<0.1% for 5218 faces), we therefore assumed element quality and quantity sufficient to produce stable solutions.

Results

Song recordings

Spectral analysis of the male calling song (Figs. 2E, S1) shows that most of the song's energy is contained within a relative narrow frequency band between ca. 8-11 kHz (pooled mean CF=9.2 ± 0.2 kHz, n=5; see also Table S1). Recordings under lab conditions exhibit an additional low amplitude frequency peak at 26-29 kHz that is not present in field recordings. As similar ultrasonic frequency

components were reported by Morris & Mason (Morris and Mason, 1995), we assume that the higher frequencies are present in all songs but attenuate quickly under field conditions.

Laser Doppler vibrometry

Pronotum resonances

LDV of the intact pronotal chamber of two living *A. acuta* males revealed two main resonance peaks at frequencies around 5 and 11 kHz (4.7 and 6 kHz, 10.4 and 11.6 kHz for Male1 and Male2 respectively; see Fig. 2A, B, E and supplementary materials Fig. S2), with vibration amplitudes of the latter being 11-22% lower than the former. Vibratory responses decline sharply after ca. 13 kHz and no additional responses can be observed in the remainder of the investigated frequency range (2-100 kHz; only frequencies up to 40 kHz are shown here). LDV of three preserved specimens present a similar picture, each showing a resonance peak between 10-12 kHz (supplementary materials Fig. S2). In addition, the preserved specimens show one or more lower frequency peaks, although the number and location of these are variable.

Wing resonances

Removal of the PC of one male (Male1) exposed the animal's forewings. As it is the case in most Tettigoniidae (Chivers et al., 2014; Morris, 1999; Richards and Davies, 1977), the left forewing lies on top of the right one and the wings are morphologically asymmetrical, with the main difference being the enlarged stridulatory file (on vein CuPb) on the left wing which is hardly developed (or 'vestigial', (Morris et al., 2016)) on the right (Fig. 2C, D).

LDV recordings of the forewings also demonstrate a clear vibratory asymmetry between left and right wings, as the right wing exhibits strongest vibratory responses at 11.5 kHz while the left wing is highly damped at this frequency, resulting in only minimal vibrations on this side (Fig. 2C, supplementary materials video 1). In contrast, at the slightly lower frequency of 10.1 kHz, the resonance properties are reversed so that the left wing is active while the right is damped (Fig. 2D). In both left and right wings, the area of vibrations is a field delineated by veins CuPb anally, CuPa costally and CuPaα laterally and bisected by vein CuPaβ, resulting in a heart-shaped vibratory pattern (venation after (Béthoux and Nel, 2001; Chivers et al., 2017)). As in the case of the PC, the left wing also shows a lower resonance peak at 6.2 kHz (Fig. 2E). The results of the LDV experiments of both PC and wings therefore show matched resonances of these two systems that coincide with the song's CF of 9.2 kHz.

Vibration of isolated pronota

To test the hypothesis of the PC functioning as a Helmholtz resonator, the pronotum of one specimen (M3, see supplementary materials Fig. S2C) was removed from the animal and scanned both on its own and with its ventral side covered with Blu-tack to mimic the presence of the abdomen closing the chamber and forming a confined space. Fig. 3 shows the vibrational responses of the dorsal part of the PC intact, removed from the animal, and covered ventrally. The intact PC exhibits, like mentioned above, pronounced resonances around 10 kHz (Fig. 3, black line) and 3 kHz that are greatly diminished when the pronotum is removed from the animal (Fig. 3, red line). Vibrational responses for the removed chamber show various lower amplitude frequency peaks from ca. 3-11 kHz and a broader resonance from ca. 17-20 kHz that are all absent in the responses from the intact chamber. When the ventral side of PC is subsequently covered with Blu-Tack to recreate the internal space previously formed by the chamber and the thorax and abdomen, the original vibratory pattern is recovered, albeit with lower amplitudes (Fig. 3, blue line). This suggests that the recorded vibrational responses from the PC of intact animals is mostly due to the chamber's internal space rather than a result of the chamber's inherent material properties alone.

Vibration of synthetic 3D printed models

To further investigate the above hypothesis, a 1:1 scale model of *A. acuta* was printed in 3D and examined with LDV as stated before for real specimens. Recorded vibrations were not as consistent over the whole area of the PC as in animal specimens but LDV-results identified an area – laterally at the posterior end, similar to the one shown in Fig. 2A – that exhibited a pronounced, sharp resonance at 11.7 kHz closely resembling results obtained from living animals (Figs. 2, 3) and a lower amplitude broader frequency response at ca. 25 kHz (Fig. 4; low frequency peaks at 3 kHz were subsequently identified as external noise through control measurements, Fig. S3).

These results provide further evidence that the resonances recorded from the PC in living animals is due to Helmholtz resonance, as the same results can be obtained with a model of the resonator that does not exhibit any of the original's material properties.

µ-CT and finite element modelling

A virtual 3D model of one *A. acuta* male was produced using data obtained from µ-CT (Fig. 5A, supplementary video 2). From this model, the volume of free space within the PC that is not occupied by the abdomen, thorax or wings, was measured to be 64.8 mm^3, with the opening of the chamber having an area of approximately 5.9 mm^2 (Fig. 5B) with an equivalent radius of 1.4 mm.

As the PC does not exhibit any neck-like opening like classical Helmholtz resonators, an end-correction term is used to modify the equation to calculate the resonance frequency f_h of a normal Helmholtz resonator

$$f_h = \frac{c}{2\pi} \cdot \sqrt{\frac{A}{Vl}}; \qquad (1)$$

to that of a neckless Helmholtz resonator

$$f_h = \frac{c}{2\pi} \cdot \sqrt{\frac{1.85r}{V}}. \qquad (2)$$

Here, c is speed of sound in air (343 m/s), A is cross-sectional area of the opening with radius r, l is the length of the neck and V denotes the volume of the resonator (Fletcher and Rossing, 1998; Rossing and Fletcher, 2012).

Using values derived from the µ-CT model in the latter equation, the resonance frequency for the PC was calculated as f_h=10.8 kHz. This value fits both with the experimental LDV results of the freely vibrating PC in response to broadband sound stimuli (10.4 and 11.6 kHz, respectively) and with the calling song CF (9.2 kHz). It also corresponds very well to resonance values obtained from experiments with isolated but ventrally closed and artificial chambers (Figs. 4, 5). Therefore, these theoretical results further support the hypothesis of the PC functioning as a Helmholtz generator.

The 3D mesh created above (Fig. 5B) served as basis for two separate, simplified linear elastic and isotropic shell models, one ventrally open (Fig. 5C) and one closed (Fig. S4). These were used in FEM to simulate the vibratory responses of both open and sealed PC in response to sound (Fig. 6).

Simulated frequency responses of the open chamber show high vibrations at 3.55 kHz, reduced vibrations at 6.15 & 10.55 kHz and a series of smaller responses upwards from ~16 kHz (Fig. 6 red line, Fig. 5C for vibration pattern at 10.55 kHz). This behaviour is not only following the general response patterns seen for the removed chamber in Fig. 3 (red line) but also shares similarities with measurements taken from intact PC (Fig. S2), where lower frequency resonances are followed by a resonance close to song frequency, being followed by either minor further responses or none. Therefore, this result illustrates a good match between the experimental measurements and the FEM simulation.

In contrast, simulated results of the closed chamber show no vibrations in the lower frequency ranges but three clear resonance peaks with decreasing amplitudes at 13.3, 22.9 and 31 kHz (Fig. 6, blue line). The observed loss of the lower frequency resonances and the abolishment of the spurious higher resonances suggest that the closed chamber approaches the function of a Helmholtz

resonator with multiple, non-harmonic resonances. The simulated first frequency peak here is with 13.3 kHz at a higher frequency than the song frequency and resonances of intact chambers (9.2 and 10-12 kHz, respectively). This might be a result of the chamber opening being too big or of mechanical constraints in the model, like the rigid seal to close the chamber dorsally, which increase overall stiffness of the system. These pronotal frequency responses as a result of FEM are again matching the experimentally determined resonances (Fig. 2A, B) and, although to a lesser degree, the mathematically calculated resonance and the general behaviour of a neckless Helmholtz resonator with similar dimensions.

Discussion

Our results show that the production of loud calling songs in *A. acuta* relies not only on the use of two, but three mechanical oscillators – the wings, the pronotal chamber possessing structural resonance, and the Helmholtz resonator formed by the chamber and the animal's body – that are set into motion and driven at or close to resonance by the animal's stridulatory movements.

The first oscillator is activated during stridulation as the movement of the scraper across the teeth on the file-bearing wing creates soundwaves through a frequency multiplication process (Bennet-Clark, 1999) at frequencies between 8-11 kHz (mean CF=9.22±0.22 kHz; Fig. 2). The sound is amplified by the wings through activation of vibratory modes close to its carrier frequency (the wing's resonance frequency, here 10.1 and 11.5 kHz for left and right wing, respectively; Fig. 2). It is rather unusual for tettigonids to exhibit two main active resonators in their wings as the highly asymmetric damping of the file-bearing left wing usually renders this wing ineffective for the radiation of sound (Montealegre-Z, 2012; Montealegre-Z and Mason, 2005; Montealegre-Z and Postles, 2010). Although, Sarria et al. (2016) described the resonances of another South-American bush-cricket, *Copiphora vigorosa*, that shows a similar shift in the resonators between right and left wings (with the resonance of the file-bearing wing being at a higher frequency) and reduced amplitudes (by ~50-75%) in the left wing (Sarria et al., 2016). In both cases, the observed wing asymmetries are not as pronounced as in other tettigonids, leading to – in comparison – less damped left wings. This tendency to wing symmetry seems to be a common feature of Tettigoniidae species with wings encapsulated by the pronotum (Morris et al., 1975). The lower resonance of the file-bearing left wing in *Acanthacara* could be explained by the added mass from the inflated file vein, while the decreased amplitude is most likely due to increased damping of the vibratory field.

In field crickets (*Gryllus bimaculatus*), where wings are more symmetric in general morphology than in tettigonids, an asymmetry in the vibration patterns of the wings can be observed as well, with lower resonances seen in the left wing than in the right (Montealegre-Z et al., 2011). However, this difference in resonance between the wings disappears when the animal is actively stridulating, with both wings converging on the lower resonance of the left wing (Montealegre-Z et al., 2011). Since the basic process of stridulation is mechanically very similar in crickets and bush-crickets, it is conceivable that the wings of *A. acuta* will likewise converge on one resonant frequency during song production.

The second resonator in the song production system is the PC in itself. Using LDV recordings on isolated PCs and FEM, we have experimentally and theoretically shown that the PC exhibits a wide range of lower frequency resonances, including one in the frequency range of the song. It is this vibratory mode that, during stridulation, will be activated to further increase the amplification of the soundwaves produced by the wings.

Furthermore, we have shown through comparisons of the intact chamber's vibratory responses with those of chambers removed from the animal's body (Figs. 3, 4), vibratory responses of artificial models (Fig. 4) and theoretical calculations and FEM (Fig. 6) that the resonance pattern of the PC changes dramatically from its intact to its removed form. When intact, it resonates as a whole at

frequencies nearly identical to the resonant frequencies of the animal's left wing (10.4 kHz and 10.1 kHz for PC and left wing, respectively; Figs. 3, S2), which is close to the song's CF and within its bandwidth. Examination of a 3D printed, artificial *Acanthacara* model using LDV produced similar results (Fig. 4), while removal of the chamber from the animal resulted in the breakdown of observed resonances and emergence of frequency responses as described above. Artificially closing the PC to mimic the state of an intact chamber was used to recreate the original frequency responses of the system. These results suggest that the overall resonant behaviour of the chamber is strongly dependent on the cavity that is formed by the chamber and the animal's thorax and abdomen (Fig. 5B) and that this behaviour is, to a certain extent, independent of the chambers material properties, which suggests a Helmholtz resonator as the basis. The theoretical calculations using the inner geometry of the chamber further document that the observed behaviour can be explained with Helmholtz resonance, while FEM substantiated this by showing that the closed model does indeed produce frequency responses like an harmonic oscillator with a fundamental resonance only slightly higher than the song frequency. These higher resonances, normally not seen in classical Helmholtz resonators, could be a result of the FEM approach, where the full numerical solution produces additional eigenfrequencies that might not be stable under real conditions (Kobayashi et al., 2009). Therefore, we propose that the third resonator in this system is the PC functioning as a Helmholtz resonator, adding more amplification and bandpass filtering to the produced song (the latter being demonstrated conclusively by (Morris and Mason, 1995)).

Having more than one resonating system for sound production is highly advantageous for small insects wanting to produce loud sounds for mate attraction as the secondary resonator does not only amplify the sound further but it also provides improved impedance matching to the surrounding air due its increased size and therefore better sound radiation (Bennet-Clark, 1999; Bennet-Clark, 2001; Fletcher, 1992). A secondary resonator can also act as a bandpass filter, restricting the frequency range of the sound coming from the first resonator. While there are multiple examples of animals using primary and secondary resonators in sound production (see introduction), the use of a tertiary resonator in animal acoustic communication has not been reported thus far. Likewise, the effect such a resonator – here in the form of the chamber resonating at the song frequency due to its own resonant properties – has on the overall amplitude and frequency component of the resulting song is largely unknown. Although, for musical instruments, like violins, it is well known that the effects of different cavity and wood resonances can be combined and coupled to produce, if not necessarily louder but richer tones (Benade, 1990; Hutchins, 1990).

To conclude, using modern imaging techniques, LDV and FEM, we show that the pronotal chamber is indeed acting as a Helmholtz resonator at the frequencies of the animals' calling song. In addition, we also show that the vibratory pattern of the pronotal chamber alone exhibits resonances in the frequency range of the calling song which allows the animal to utilise not two but three coupled resonators for sound production, amplification and radiation.

Authors' contributions

F.M-Z., and T.J. conceived and designed the experiments. F.M-Z., B.C, F.S and T.J. performed the experiments. KR-B performed µCT scans and processed X-ray images for further analysis. F.M-Z and T.J. analysed data. T.J. performed 3D and FEM modelling. T.J. and F.M-Z. wrote the manuscript. M.W. processed and produced 3D printed models for experimentation. All authors reviewed the manuscript.

Competing interests

The authors have declared that no competing interests exist.

Funding

F.M-Z, T.J. and B.C. are currently funded by the Leverhulme Trust (grant No. RPG-2014-284).

Acknowledgements

The authors wish to thank the editor and two anonymous reviewers for their valuable comments that greatly improved the quality and clarity of the paper.

References

Benade, A. H. (1990). Fundamentals of musical acoustics: Courier Corporation.

Bennet-Clark, H. and Young, D. (1994). The scaling of song frequency in cicadas. *Journal of Experimental Biology* **191**, 291-294.

Bennet-Clark, H. C. (1987). The Tuned Singing Burrow of Mole Crickets. *Journal of Experimental Biology* **128**, 383-409.

Bennet-Clark, H. C. (1998). Size and scale effects as constraints in insect sound communication. *Philosophical Transactions of the Royal Society of London Series B-Biological Sciences* **353**, 407-419.

Bennet-Clark, H. C. (1999). Resonators in insect sound production: how insects produce loud pure-tone songs. *Journal of Experimental Biology* **202**, 3347-3357.

Bennet-Clark, H. C. (2001). Impedance Matching in Sound Production and Hearing: a Comparative Study. In *Ecology of Sensing*, eds. F. G. Barth and A. Schmid), pp. 39-58. Berlin, Heidelberg: Springer Berlin Heidelberg.

Bennet-Clark, H. C. (2003). Wing resonances in the Australian field cricket Teleogryllus oceanicus. *Journal of Experimental Biology* **206**, 1479-1496.

Béthoux, O. and Nel, A. (2001). Venation pattern of Orthoptera. *Journal of Orthoptera Research* **10**, 195-198.

Braun, H., Chamorro-Rengifo, J. and Morris, G. K. (2009). Curious Katydids from the Andes of Colombia and Ecuador: Three New Species, a New Genus and Acoustic Baffles. *Journal of Orthoptera Research* **18**, 225-235.

Chivers, B. D., Béthoux, O., Sarria-S, F. A., Jonsson, T., Mason, A. C. and Montealegre-Z, F. (2017). Functional morphology of tegmina-based stridulation in the relict species *Cyphoderris monstrosa* (Orthoptera: Ensifera: Prophalangopsidae). *Journal of Experimental Biology*.

Chivers, B. D., Jonsson, T., Cadena-Castaneda, O. J. and Montealegre-Z, F. (2014). Ultrasonic reverse stridulation in the spider-like katydid *Arachnoscelis* (Orthoptera: Listrosceledinae). *Bioacoustics* **23**, 67-77.

Chivers, B. D., Jonsson, T., Jackson, J. C., Kleinhappel, T. K., Shivarova, N., Windmill, J. F. C. and Montealegre-Z, F. (2015). Distribution of sound pressure around a singing cricket: radiation pattern and asymmetry in the sound field. *Bioacoustics*, 1-16.

Drosopoulos, S. and Claridge, M. F. (2006). Insect Sounds and Communication: Physiology, Behaviour, Ecology and Evolution: CRC Press.

Fletcher, N. (2007). Animal Bioacoustics. In *Springer Handbook of Acoustics*, (ed. T. D. Rossing), pp. 785-804. New York, NY: Springer.

Fletcher, N. H. (1992). Acoustic systems in biology: Oxford University Press.

Fletcher, N. H. and Rossing, T. (1998). The Physics of Musical Instruments. New York: Springer.

Fletcher, N. H. and Tarnopolsky, A. (1999). Acoustics of the avian vocal tract. *Journal of the Acoustical Society of America* **105**, 35-49.

Gurney, A. B. (1972). The South American Katydid Genus *Acanthacara*: Descriptive Notes And Subfamily Position (Orthoptera: Tettigoniidae Agraeciinae). *Journal of Washington Academy of Sciences* **62**.

Hauser, M. D. (2000). The evolution of communication. Cambridge, Mass.: MIT Press.

Hedwig, B. (2014). Insect hearing and acoustic communication: Springer Berlin Heidelberg.

Heller, K. G., Ostrowski, T. D. and Hemp, C. (2010). Singing and Hearing in *Aerotegmina kilimandjarica* (Tettigoniidae: Hexacentrinae), a Species with Unusual Low Carrier Frequency of the Calling Song. *Bioacoustics* **19**, 195-210.

Hutchins, C. M. (1990). A study of the cavity resonances of a violin and their effects on its tone and playing qualities. *Journal of the Acoustical Society of America* **87**, 392-397.

Kalmring, K., Jatho, M., Hoffmann, E., Stiedl, O., Schul, J., Schröder, H., Stephens, R. and Hartley, C. (2003). The Auditory-Vibratory Sensory System in Bushcrickets (Tettigoniidae, Ensifera, Orthoptera) II. Signal Production and Acoustic Behavior. In *Environmental Signal Processing and Adaptation*, eds. G. Heldmaier and D. Werner), pp. 209-232. Berlin, Heidelberg: Springer Berlin Heidelberg.
Klocke, D. and Schmitz, H. (2011). Water as a major modulator of the mechanical properties of insect cuticle. *Acta Biomaterialia* **7**, 2935-2942.
Kobayashi, T., Takami, T., Miyamoto, M., Takahashi, K. y., Nishida, A. and Aoyagi, M. (2009). 3D calculation with compressible LES for sound vibration of Ocarina. *arXiv preprint arXiv:0911.3567*.
Lardner, B. and bin Lakim, M. (2002). Animal communication: Tree-hole frogs exploit resonance effects. *Nature* **420**, 475-475.
Malkin, R., McDonagh, T. R., Mhatre, N., Scott, T. S. and Robert, D. (2014). Energy localization and frequency analysis in the locust ear. *Journal of Royal Society Interface* **11**.
Marten, K., Quine, D. and Marler, P. (1977). Sound transmission and its significance for animal vocalization: II. Tropical forest habitats. *Behavioral Ecology and Sociobiology* **2**, 291-302.
Masaki, S., Kataoka, M., Shirato, K. and Nakagahara, M. (1987). Evolutionary differentiation of right and left tegmina in crickets. In *Evolutionary biology of orthopteroid insects*, (ed. B. M. Baccetti). Chichester: Ellis Horwood Limited.
Montealegre-Z, F. (2009). Scale effects and constraints for sound production in katydids (Orthoptera: Tettigoniidae): correlated evolution between morphology and signal parameters. *Journal of Evolutionary Biology* **22**, 355-66.
Montealegre-Z, F. (2012). Reverse stridulatory wing motion produces highly resonant calls in a neotropical katydid (Orthoptera: Tettigoniidae: Pseudophyllinae). *Journal of Insect Physiology* **58**, 116-124.
Montealegre-Z, F., Jonsson, T. and Robert, D. (2011). Sound radiation and wing mechanics in stridulating field crickets (Orthoptera: Gryllidae). *Journal of Experimental Biology* **214**, 2105-17.
Montealegre-Z, F. and Mason, A. C. (2005). The mechanics of sound production in *Panacanthus pallicornis* (Orthoptera : Tettigoniidae : Conocephalinae): the stridulatory motor patterns. *Journal of Experimental Biology* **208**, 1219-1237.
Montealegre-Z, F. and Postles, M. (2010). Resonant Sound Production in *Copiphora gorgonensis* (Tettigoniidae: Copiphorini), an Endemic Species from Parque Nacional Natural Gorgona, Colombia. *Journal of Orthoptera Research* **19**, 347-355.
Morris, G. (1999). Song in arthropods. In *Encyclopedia of Reproduction*, eds. E. Knobil and J. Neill), pp. 508-517. San Diego: Academic Press.
Morris, G. and Mason, A. (1995). Covert stridulation: novel sound generation by a South American katydid. *Naturwissenschaften* **82**, 96-98.
Morris, G. K., Aiken, R. B. and Kerr, G. E. (1975). Calling Songs of *Neduba macneilli* and *N. sierranus* (Orthoptera: Tettigoniidae: Decticinae). *Journal of the New York Entomological Society* **83**, 229-234.
Morris, G. K., Braun, H. and Wirkner, C. S. (2016). Stridulation of the clear-wing meadow katydid *Xiphelimum amplipennis*, adaptive bandwidth. *Bioacoustics* **25**, 225-251.
Prestwich, K. N. (1994). The Energetics of Acoustic Signaling in Anurans and Insects. *American Zoologist* **34**, 625-643.
Rentz, D. (1988). The shield-backed katydids of Southern Africa: their taxonomy, ecology and relationships to the faunas of Australia and South America (Orthoptera : Tettigoniidae : Tettigoniinae). *Invertebrate Systematics* **2**, 223-335.
Richards, O. W. and Davies, R. G. (1977). Orthoptera (Grasshoppers, Locusts, Crickets, Etc.). In *Imms' General Textbook of Entomology: Volume 2: Classification and Biology*, pp. 537-561. Dordrecht: Springer Netherlands.

Robinson, D. J. and Hall, M. J. (2002). Sound signalling in Orthoptera. *Advances in Insect Physiology* **29**, 151-278.
Rossing, T. and Fletcher, N. H. (2012). Principles of Vibration and Sound: Springer.
Sarria, S. F. A., Buxton, K., Jonsson, T. and Montealegre-Z, F. (2016). Wing mechanics, vibrational and acoustic communication in a new bush-cricket species of the genus *Copiphora* (Orthoptera: Tettigoniidae) from Colombia. *Zoologischer Anzeiger* **263**, 55-65.
Smith, C. W., Herbert, R., Wootton, R. J. and Evans, K. E. (2000). The hind wing of the desert locust (*Schistocerca gregaria* Forskal). II. Mechanical properties and functioning of the membrane. *Journal of Experimental Biology* **203**, 2933-2943.
Vincent, J. F. V. and Wegst, U. G. K. (2004). Design and mechanical properties of insect cuticle. *Arthropod Structure & Development* **33**, 187-199.
von Helmholtz, H. (1863). Die Lehre von den Tonempfindungen als physiologische Grundlage für die Theorie der Musik. Braunschweig: F. Vieweg und Sohn.

Figures

Fig. 1. *Acanthacara acuta* male. Photograph of a live *A. acuta* male taken in its natural habitat at Santa Lucía Cloud Forest Reserve, Ecuador, September 2014 by FMZ. The pronotum with its inflated part forming the pronotal chamber measures ca. 10 mm, covers the whole of the thorax, the brachypterous wings, and the first abdominal segment.

Journal of Experimental Biology • Advance article

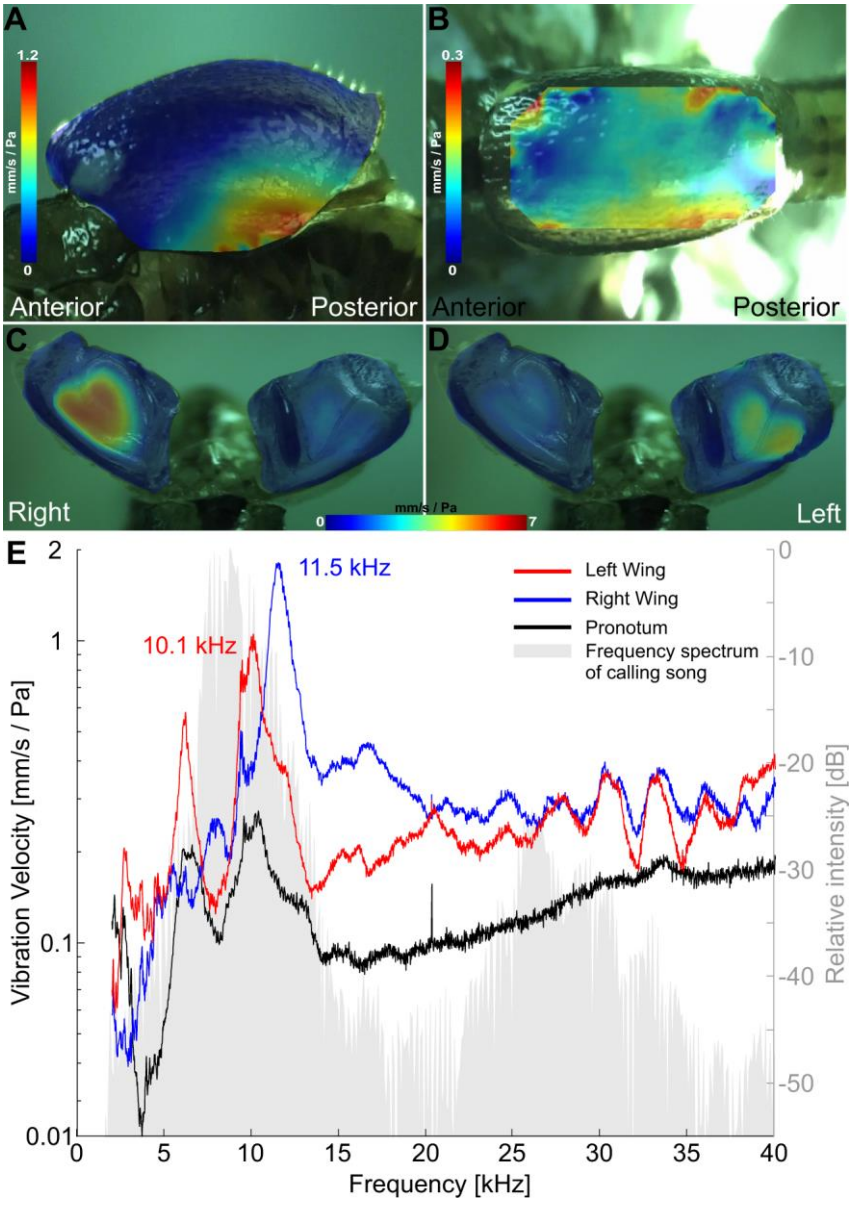

Fig. 2. Analysis of vibratory properties of the wings and pronotal chamber of a male *A. acuta*. (A-D) Vibration maps of pronotal chamber in lateral and dorsal view (A, B) and right and left forewings (C, D), showing vibration velocities at resonance as measured by LDV (f_0=10.4 kHz for a, b), f_0=11.5 kHz for C and f_0=10.1 kHz for D). Relative vibration velocities (in mm/s / Pa) represented by colours with highest amplitudes in red and no vibrations in blue. (E) FFT of the vibratory response for wings (blue=right, red=blue) and pronotal chamber (black). Frequency spectrum of a calling song pulse in light grey.

Journal of Experimental Biology • Advance article

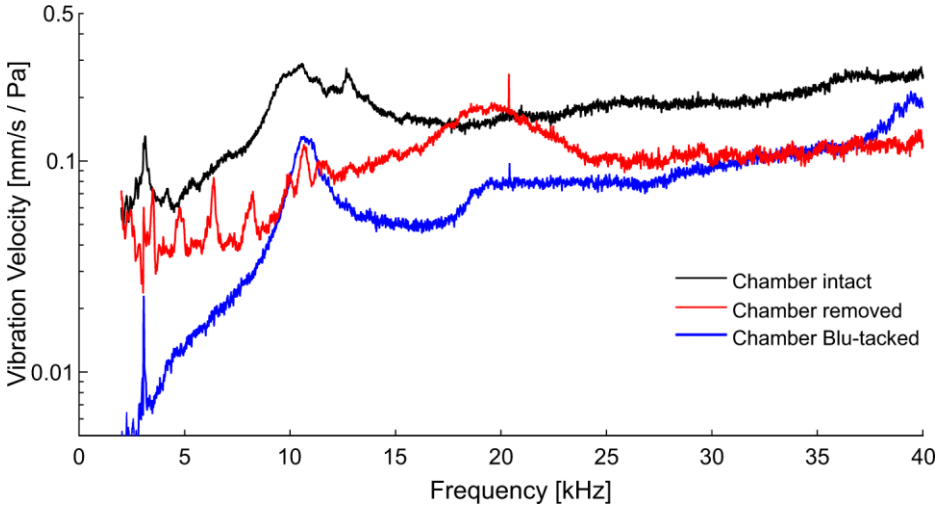

Fig. 3. Vibrational responses to broadband chirps of one *A. acuta* pronotal chamber for three treatments. Black: intact chamber; red: chamber removed; blue: chamber ventrally covered to recreate the effect of thorax and abdomen.

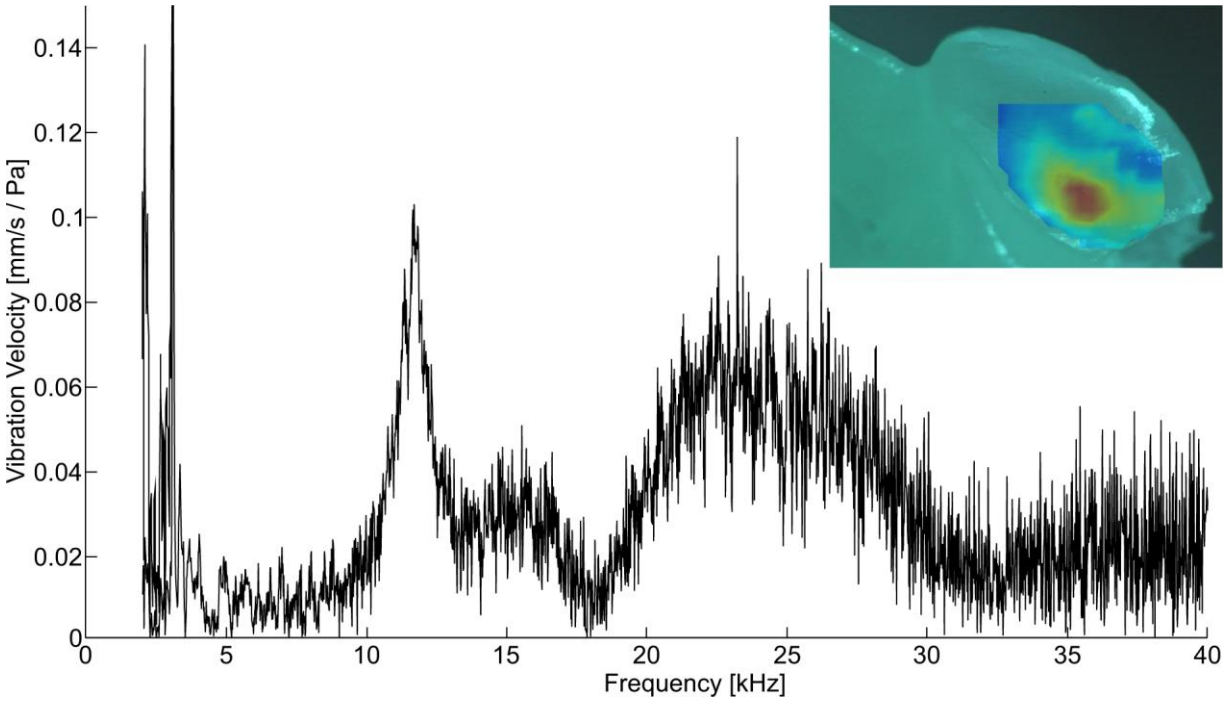

Fig. 4. Single point vibrational response of the pronotal chamber of a 1:1 scale model of *A. acuta*. The inset shows the model and a map of vibrations at the peak frequency of 11.7 kHz.

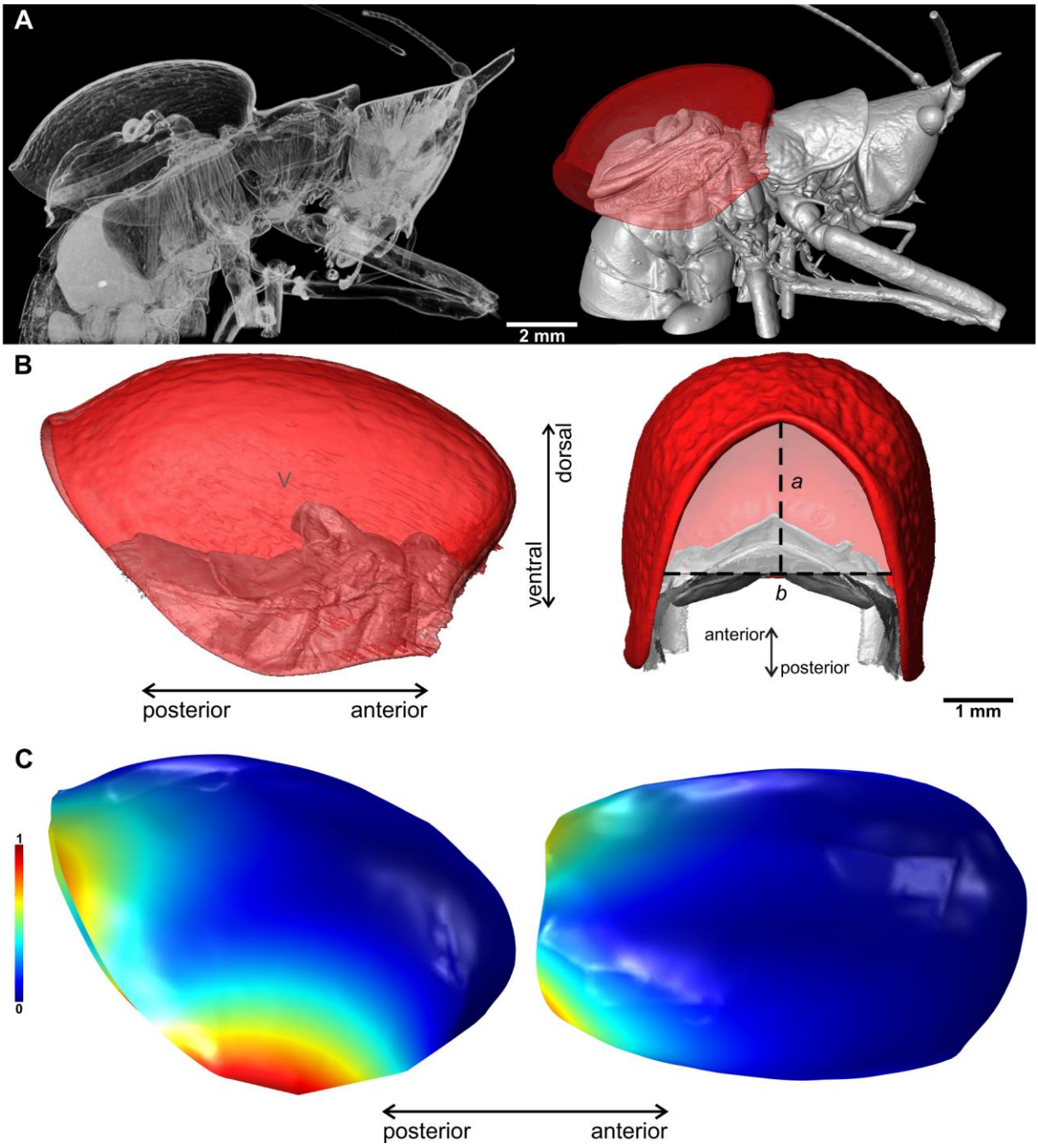

Fig. 5. 3D reconstructions of a male of *A. acuta*. (A) Sagittal cross-section (left) and 3D model with transparent pronotal chamber in red (right). (B) Lateral view of right side (left) and posterior view (right) of pronotal chamber without wings. Dorsal cuticle of abdomen and thorax in grey. Dashed lines *a*, *b* denote axes used to approximate the area of the pronotal chamber opening. (C) Lateral (left) and dorsal (right) view of PC model used for FEM showing relative surface displacement at the second vibratory mode at 10.55 kHz.

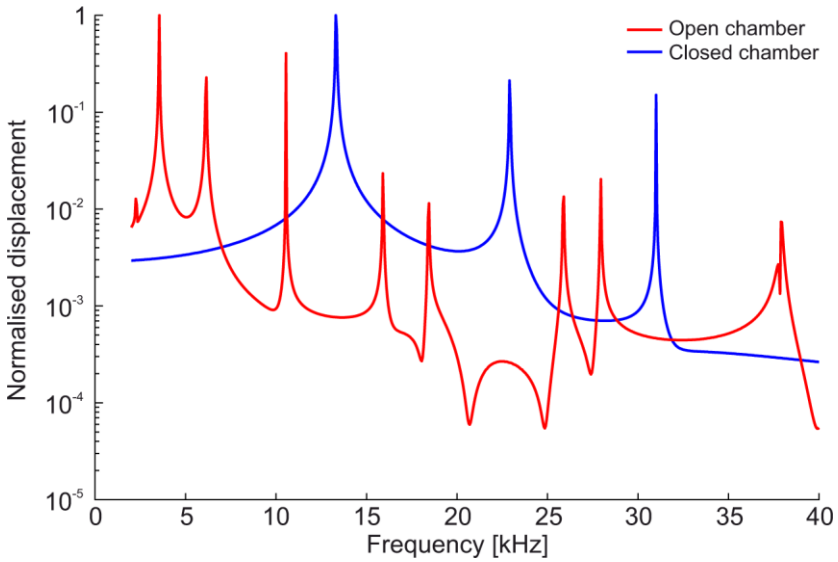

Fig. 6. Simulated vibrational response to a range of sound frequencies (from 2-40 kHz at 50 Hz steps) of the pronotal chamber model in both open (red) and closed (blue) state. Vibration velocities are normalised between 0-1 for each simulation.

Supplementary Materials

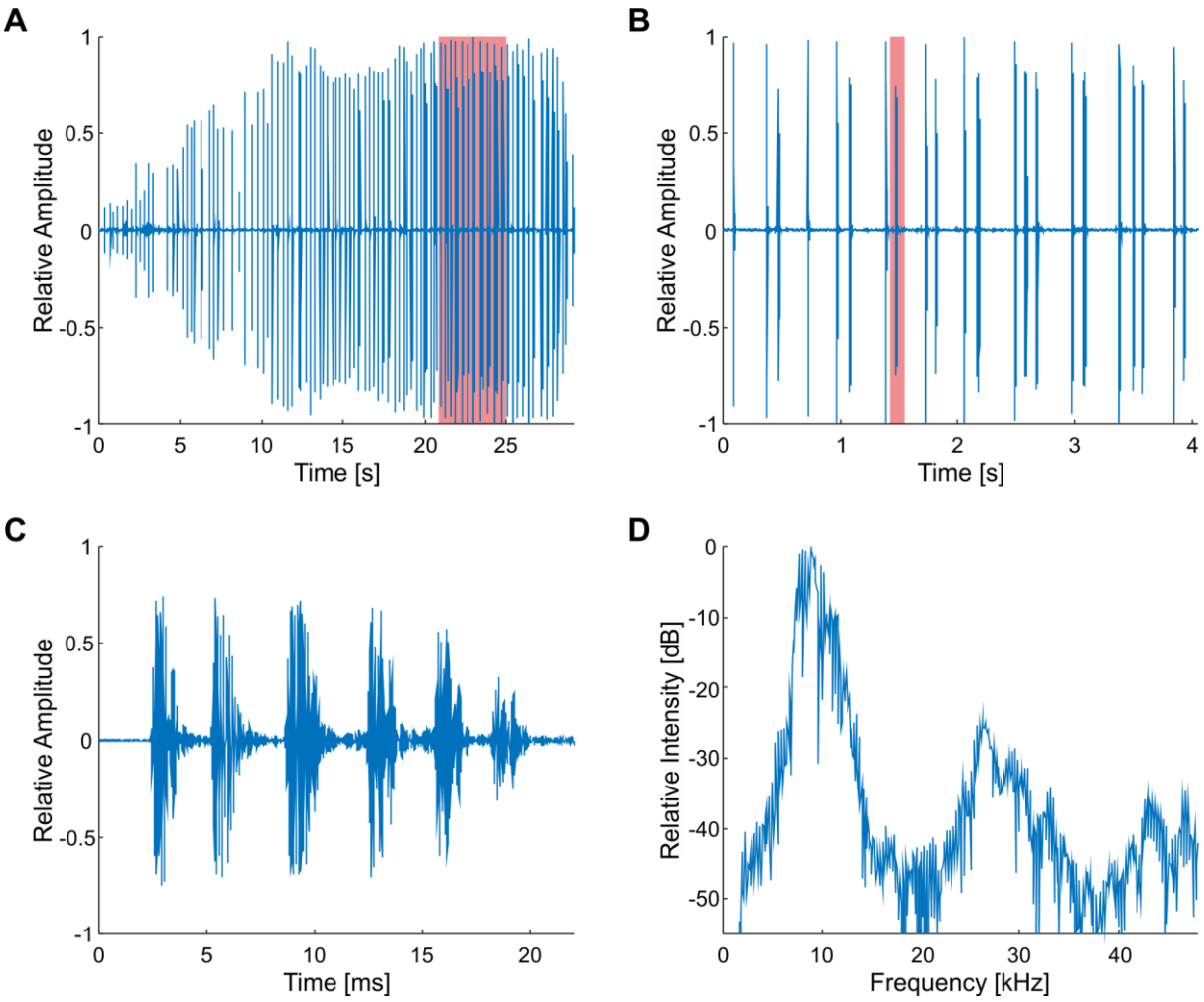

Fig. S1. *Acanthacara acuta* male song as recorded under lab conditions. (A) Continuous calling song consisting of long train of individual pulses. (B) Group of pulses taken from shaded area in A. (C) Magnification of pulse in shaded area in B, showing six separate impulses. (D) Frequency spectrum of pulse in B, C, showing main song energy in a frequency band between 8-11 kHz (peak at 8.8 kHz) and a low amplitude frequency band between 25-28 kHz.

Table S1: Individual results from song parameter analysis. CF = pulse carrier frequency, n = number of pulses, PL = pronotal length (measured as proxy of body size from anterior to posterior part of the pronotum, including the pronotal chamber itself), SD = standard deviation. *Animal recordings performed under lab conditions rather than field recordings. The pooled mean was calculated as: $\bar{X} = \frac{\sum_i n_i x_i}{\sum_i n_i}$; with *x* being individual averages and *n* the numbers of observations in each average. The pooled standard deviation was calculated as: $\sigma_p = \sqrt{\frac{\sum_i (n_i - 1)\sigma_i^2}{\sum_i (n_i - 1)}}$; with σ being the individual standard deviations.

	PL [mm]	*CF [kHz]*	*SD [kHz]*	*n*
M1	*10.54*	*9.48*	*0.40*	*90*
M2	*10.56*	*10.33*	*0.37*	*252*
M3	*10.18*	*9.04*	*0.12*	*876*
M4	*10.05*	*8.90*	*0.19*	*398*
M5*	*10.03*	*9.04*	*0.30*	*118*
Pooled mean		*9.22*	*0.22*	*-*

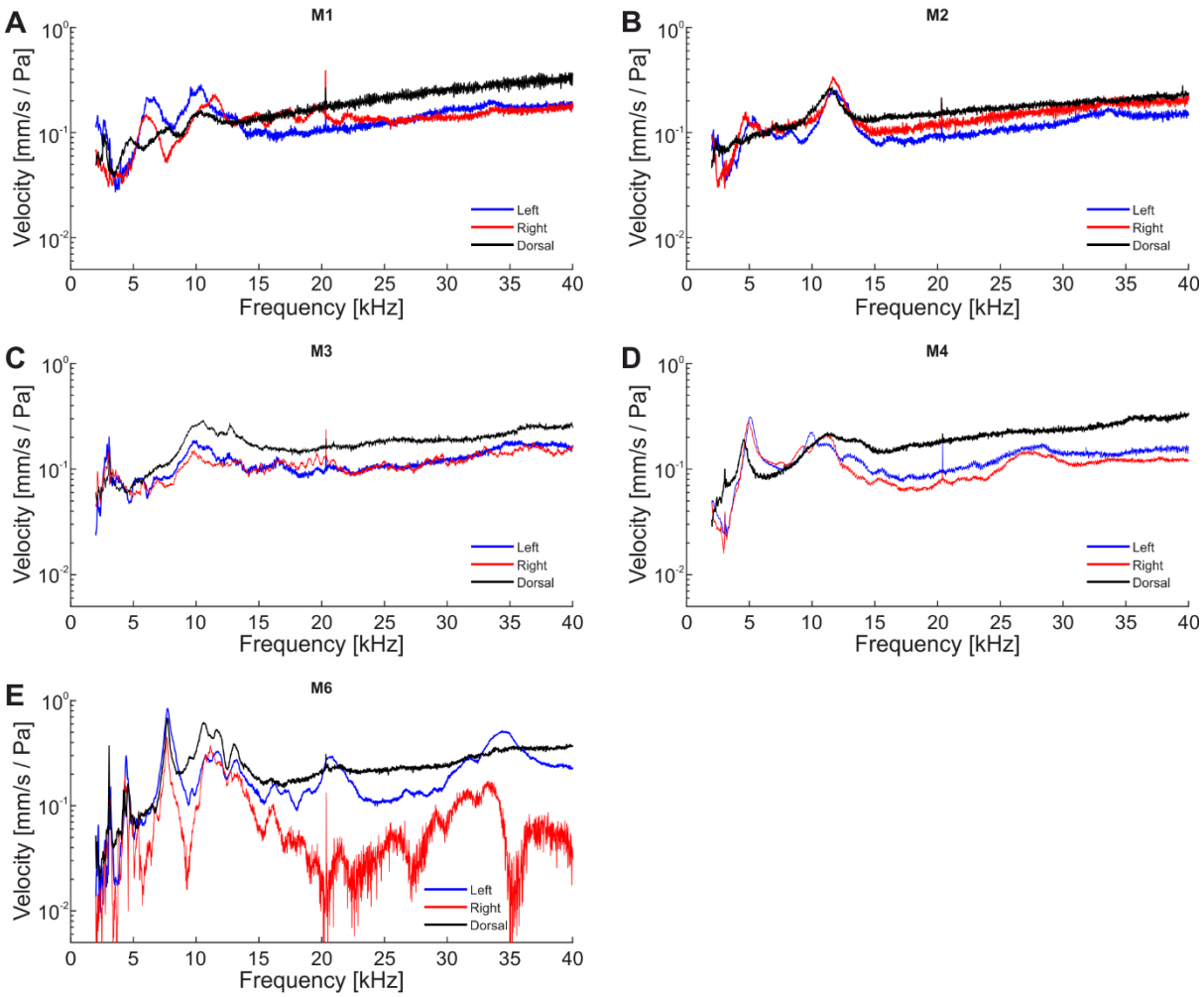

Fig. S2. Frequency analysis of the vibratory displacement of 5 male A. acuta intact pronotal chambers in response to broadband periodic chirps (2-100 kHz, only frequencies up to 40 kHz shown here). Chambers were scanned from both lateral sides (blue and red lines) and dorsally. Values are normalised to the maximum displacement for each specimen. A-D shows recordings from live specimens, while E shows data from a dried and pinned specimen.

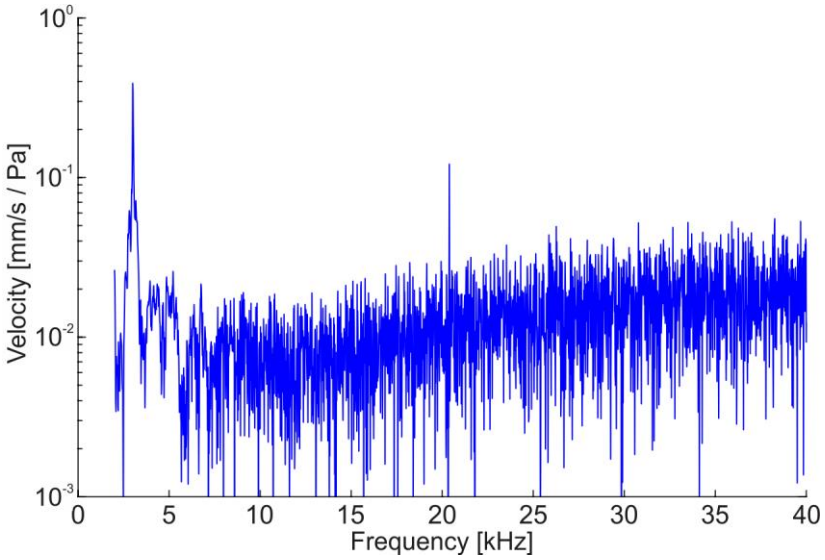

Fig. S3: LDV control recording on for the vibrational responses of the printed pronotal chamber. The laser was focussed on a holder in the experimental setup and no sound was played. This shows an underlying 3 kHz vibration present in the anechoic chamber on this particular recording day (probably due to building noise).

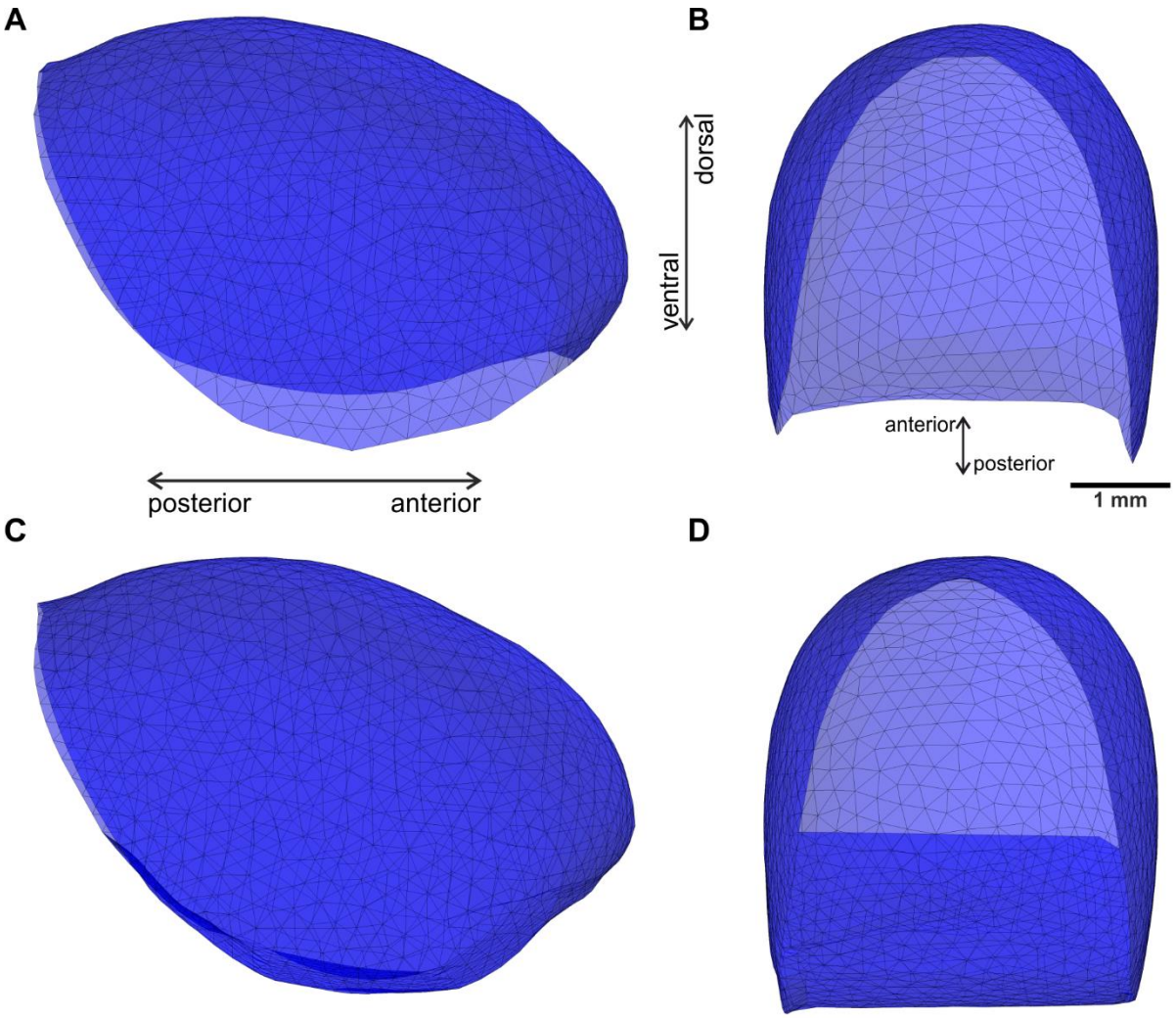

Fig. S4: Overview of the two different 3D mesh models of the pronotal chamber of A. acuta used as basis for finite element modelling. (A, B) lateral and posterior-anterior view of the open chamber mesh. (C, D) lateral and posterior-anterior view of the closed chamber mesh.

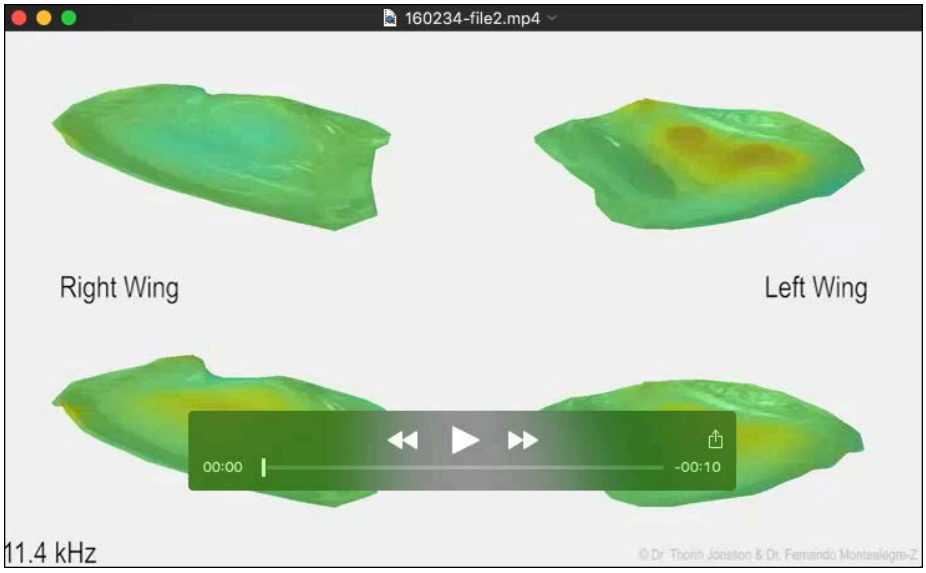

Supplementary video 1: Video showing a frontal view of the vibratory patterns of the forewings of a male *Acanthacara acuta* as recorded with laser Doppler vibrometry. The top half shows vibration amplitudes of both wings at the left wing's resonance (10.1 kHz), the bottom half at the right wing's resonance (11.4 kHz, see also Fig.2).

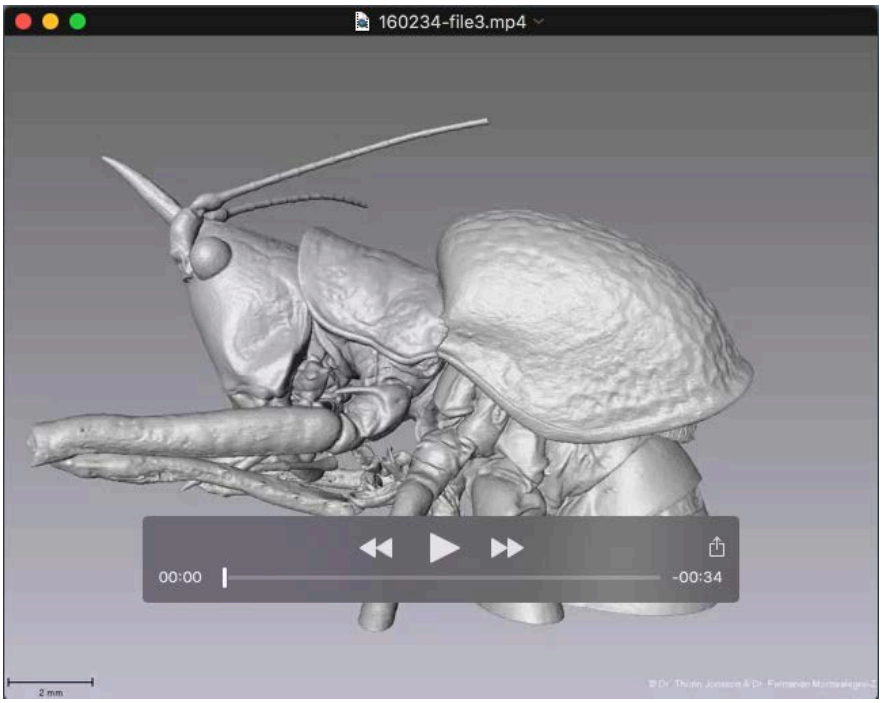

Supplementary video 2: Video of a male *Acanthacara acuta* as modelled from µ-CT scans with a focus on the pronotal chamber and wings.